5-19-2011

Surrogate Measurement of the ^{238}Pu(n,f) Cross Section

J. J. Ressler

J. T. Burke

J. Escher

C. Angell

M. S. Basunia

See next page for additional authors

Recommended Citation

Ressler, J., J. Burke, J. Escher, C. Angell, M. Basunia, C. Beausang, L. Bernstein, D. Bleuel, R. Casperson, B. Goldblum, J. Gostic, R. Hatarik, R. Henderson, R. Hughes, J. Munson, L. Phair, T. Ross, N. Scielzo, E. Swanberg, I. Thompson, and M. Wiedeking. "Surrogate Measurement of the ^{238}Pu(n,f) Cross Section." *Physical Review C* 83, no. 5 (May 19, 2011): 054610: 1-54610: 7. doi:10.1103/PhysRevC.83.054610.

Authors
J. J. Ressler, J. T. Burke, J. Escher, C. Angell, M. S. Basunia, C. W. Beausang, L. A. Bernstein, D. L. Bleuel, R. J. Casperson, B. L. Goldblum, J. Gostic, R. Hatarik, R. Henderson, R. O. Hughes, J. Munson, L. Phair, T. J. Ross, N. D. Scielzo, E. Swanberg, I. Thompson, and M. Wiedeking

Surrogate measurement of the ^{238}Pu(n,f) cross section

J. J. Ressler,[1,*] J. T. Burke,[1] J. E. Escher,[1] C. T. Angell,[2] M. S. Basunia,[3] C. W. Beausang,[4] L. A. Bernstein,[1] D. L. Bleuel,[1] R. J. Casperson,[1] B. L. Goldblum,[2,†] J. Gostic,[1] R. Hatarik,[1,3] R. Henderson,[1] R. O. Hughes,[4] J. Munson,[2] L. W. Phair,[3] T. J. Ross,[4,5] N. D. Scielzo,[1] E. Swanberg,[1,2] I. J. Thompson,[1] and M. Wiedeking[1]

[1]*Lawrence Livermore National Laboratory, Livermore, California 94551, USA*

[2]*Department of Nuclear Engineering, University of California, Berkeley, California 94720, USA*

[3]*Lawrence Berkeley National Laboratory, Berkeley, California 94720, USA*

[4]*Department of Physics, University of Richmond, Richmond, Virginia 23173, USA*

[5]*Department of Physics, University of Surrey, Guildford GU2 7XH, United Kingdom*

(Received 12 January 2011; published 19 May 2011)

The neutron-induced fission cross section of ^{238}Pu was determined using the surrogate ratio method. The (n,f) cross section over an equivalent neutron energy range 5–20 MeV was deduced from inelastic α-induced fission reactions on ^{239}Pu, with ^{235}U$(\alpha,\alpha' f)$ and ^{236}U$(\alpha,\alpha' f)$ used as references. These reference reactions reflect ^{234}U(n,f) and ^{235}U(n,f) yields, respectively. The deduced ^{238}Pu(n,f) cross section agrees well with standard data libraries up to ∼10 MeV, although larger values are seen at higher energies. The difference at higher energies is less than 20%.

DOI: 10.1103/PhysRevC.83.054610 PACS number(s): 24.87.+y, 25.85.Ge, 24.10.−i, 25.40.Lw

I. INTRODUCTION

As part of a larger effort to reduce carbon emissions and the reliance on foreign imports, support for alternative power sources, including nuclear, has been growing in the United States. The Energy Policy Act of 2005 and Nuclear Power 2010 Program support the development of new nuclear power plants. The proposed plants are based on similar designs to the current fleet, but offer improvements in safety and efficiency. A similar resurgence has been seen internationally, with new reactors being built in South America, Asia, Africa, and Europe. In 2010, Germany reversed a decision to shut down reactors [1], and Sweden followed suit in June [2].

The renewed interest in nuclear power has led to a number of novel materials proposed for fuels and reactor components. Future designs have been consolidated into six candidates for further development [3]. These generation-IV (Gen-IV) reactors advertise enhanced safety, reliability, and sustainability. In addition, the new designs promote proliferation resistance and waste reduction. While the very high temperature reactor (VHTR) will use thermal neutrons for energy production, the remaining five [supercritical water cooled (SCWR), molten salt reactor (MSR), gas-cooled fast reactor (GFR), sodium-cooled fast reactor (SFR), and lead-cooled fast reactor (LFR)] may utilize fast neutrons. Accurate data sets, notably neutron-induced cross sections, are vital to the engineering and design of these systems.

Fast neutron reactions have also been proposed for the incineration of actinide material, notably the minor actinide isotopes of Np, Am, and Cm. Spent fuel will be burned in a dedicated reactor where neutron reactions such as (n,f) or $(n,2n)$ may be used to reduce the content of radiotoxic isotopes.

A number of new or improved neutron measurements are needed to determine the feasibility, effectiveness, and safety issues for the novel engineering efforts proposed for these applications. Data collection is often hampered by the need for radioactive targets; the use of such targets is limited to longer-lived isotopes due to the large background induced by the decay of the material.

Near stability, alternate or "surrogate" reactions can be used to determine cross sections for isotopes of interest. In the actinide region, short-lived isotopes often have longer-lived neighbors. Charged particle reactions on these neighboring isotopes can be used to form the same compound nucleus as the desired reaction. Decay from the compound state is assumed to be independent of the production mechanism, allowing reactions with the neighboring isotopes to be used as a surrogate for the neutron-induced reaction of interest.

We have recently measured the neutron-induced fission cross section of ^{238}Pu, performed via the surrogate reaction ^{239}Pu$(\alpha,\alpha' f)$. The neutron-induced fission cross section of ^{238}Pu is needed for reactor applications, particularly the sodium fast reactor, as well as transmutation schemes. Few measurements have been performed, resulting in sparse data above 5 MeV. Figure 1 shows (n,f) cross section data from EXFOR for neutron energies above 1 MeV.

The lack of higher-energy data results in large uncertainties for the tabulated data. The recent Japanese Evaluated Nuclear Data Library (JENDL-4) includes covariance data for neutron cross sections. For ^{238}Pu(n,f), the uncertainty in the cross section above 5 MeV is ∼3.5%, and >5% above 10 MeV. The JENDL recommended cross section, with uncertainty, is shown with other major data libraries in Fig. 2 .

In the current work, the ^{238}Pu(n,f) cross section was deduced from 5 to 20 MeV in a single measurement using the ^{239}Pu$(\alpha,\alpha' f)$ surrogate reaction. The use of induced

*ressler2@llnl.gov

†Present address: Department of Nuclear Engineering, University of Tennessee, Knoxville, Tennessee 37996, USA.

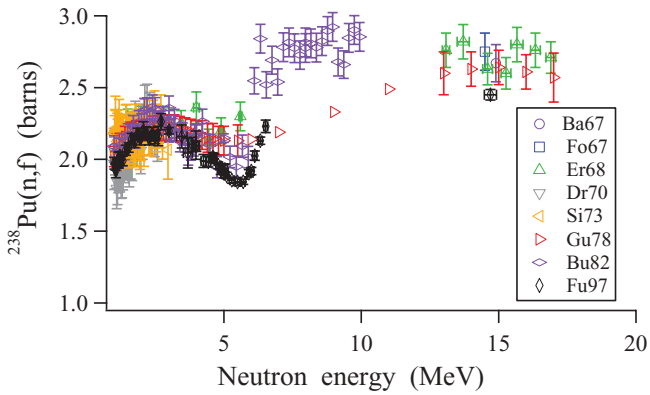

FIG. 1. (Color online) Neutron-induced fission cross sections for ^{238}Pu. Data are from Refs. [4–11].

fission by α inelastic scatter as a surrogate for (n,f) reactions has been recently benchmarked with uranium isotopes near $A \sim 235$ [12].

II. SURROGATE RATIO METHOD

The surrogate method was introduced in 1970, utilizing (t,p) reactions to determine (n,f) cross sections for Th, U, and Pu isotopes [13]. More recently, a variety of charged particle reactions have been successfully used to determine (n,f), cross sections for a broad range of actinide nuclei [14–21].

The correlation between the neutron-induced and surrogate reaction is built upon a Hauser-Feshbach formalism to describe the compound reaction. For simplicity, the decay probablity of the compound nucleus is assumed to be independent of the angular momentum and parity of the populated states. This assumption is the Weisskopf-Ewing limit, and often works well for (n,f) cross sections at higher equivalent neutron energies ($\gtrsim$5 MeV). At lower energies, the Weisskopf-Ewing assumption fails and differences between the spin-parity populations in the desired and surrogate reactions have to be accounted for. Within the Weisskopf-Ewing limit, the neutron-induced fission cross section is equal to the product

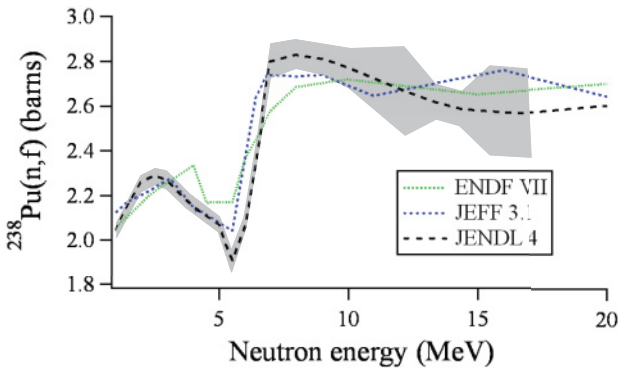

FIG. 2. (Color online) Neutron-induced fission cross sections for ^{238}Pu from select data libraries. For ^{238}Pu(n,f), ENDF-VI and ENDF-VII data are equivalent, as are JEFF-3.1 and JENDL-3.3 for neutron energies above 1 MeV. The shaded area represents the cross-section uncertainty from the covariance data in JENDL-4.

of the formation cross section for the compound nucleus using a neutron reaction (σ_{CN}) and the probability for the decay channel using the charged particle surrogate reaction (P) [22]. For the α-induced fission surrogate reaction,

$$\sigma_{(n,f)} = \sigma_{CN} P_{(\alpha,\alpha' f)}. \tag{1}$$

The formation cross sections can typically be calculated using an optical model potential to a greater accuracy than the decay probability. However, the decay probability can be readily measured. The α-induced fission probability ($P_{(\alpha,\alpha' f)}$) as a function of compound nuclear excitation energy is

$$P_{(\alpha,\alpha' f)} = \frac{N_{(\alpha,\alpha' f)}}{\varepsilon_f N_\alpha}, \tag{2}$$

where $N_{(\alpha,\alpha' f)}$ and N_α are the number of detected α-fission coincidences and total number of detected α scatter reactions, respectively, and ε_f is the fission detection efficiency. The total number of observed direct α scatter reactions is determined by the product of the direct reaction cross section (σ_α), the α-detection efficiency (ε_α), the areal target density (ρ_T), the live time fraction (ℓ_t), and the integrated charge delivered by the particle beam (Q) over the course of the experiment:

$$N_\alpha = \varepsilon_\alpha \rho_T \ell_t Q \sigma_\alpha. \tag{3}$$

For the actinide isotopes, determination of the total number of direct reaction events (N_α) is complicated by impurities. Most actinides readily form oxides and materials are typically not self-supporting, requiring the use of carbon or metal backings.

To reduce the effects of contaminants, the surrogate ratio method (SRM) has been used. This technique determines the ratio of an unknown cross section relative to a known one, and is described in detail in Refs. [12,22] for surrogate (n,f) reactions. If the experimental set up does not change for the two reactions, the detection efficiencies (ε_α and ε_f) can often be assumed to be the same. For reactions on similar nuclei, the direct cross sections (σ_α) may also be nearly equal. The ratio of an unknown (unk) to known, or reference (ref), cross section as a function of energy for the α-induced surrogate reaction is, therefore, denoted as

$$\frac{\sigma_{(n,f),\mathrm{unk}}}{\sigma_{(n,f),\mathrm{ref}}} = C \frac{\sigma_{CN,\mathrm{unk}}}{\sigma_{CN,\mathrm{ref}}} \frac{N_{(\alpha,f),\mathrm{unk}}}{N_{(\alpha,f),\mathrm{ref}}} \tag{4}$$

within the Weisskopf-Ewing limit. The constant C is energy independent and is equal to

$$C = \frac{\rho_{T,\mathrm{ref}}}{\rho_{T,\mathrm{unk}}} \frac{\ell_{t,\mathrm{ref}}}{\ell_{t,\mathrm{unk}}} \frac{Q_{\mathrm{ref}}}{Q_{\mathrm{unk}}} \tag{5}$$

under the assumptions that the detection efficiencies and direct reaction cross sections are equal for the reference and unknown systems.

In the current experiment, the ^{238}Pu(n,f) cross section was determined via ratios with ^{234}U(n,f) and ^{235}U(n,f). Table I highlights relevant characteristics for each reaction.

While the ^{235}U(n,f) cross section is very well known, with uncertainties $<$1%, the large difference in neutron separation energy and the odd/even effect for the neutron number of the

TABLE I. Desired and surrogate reactions used in the determination of ^{238}Pu(n,f). Also shown are the ground-state spins and parities for the surrogate isotope, with the neutron separation energy.

Reaction	Surrogate	J^π	S_N (MeV)
^{238}Pu(n,f)	^{239}Pu$(\alpha,\alpha' f)$	$1/2^+$	5.2
^{234}U(n,f)	^{235}U$(\alpha,\alpha' f)$	$7/2^-$	5.6
^{235}U(n,f)	^{236}U$(\alpha,\alpha' f)$	0^+	6.2

surrogate isotopes may limit the model independence desired by the use of the SRM. The nuclear structure of the ^{234}U(n,f) surrogate is more similar to the unknown reaction, although the spin difference is significant ($\Delta J = 3$) and the (n,f) cross section is less well known ($\sim$3%) for fast neutrons.

The experimental configuration is described below, with results for the new measurement.

III. EXPERIMENT

Thin actinide targets were prepared by electrodepositing isotopically enriched material on 100-μg/cm^2 natural carbon foils. An electroplating cell was designed to allow direct deposition of thin actinide films within a confined area on a target frame. The areal density of each target was determined by α counting. For the current work, targets of 140(8)-μg/cm^2 ^{239}Pu, 416(23)-μg/cm^2 ^{235}U, and 322(18)-μg/cm^2 ^{236}U were prepared. For all three targets, contaminant species (e.g., ^{234}U, ^{238}Pu) were less than 1%.

The actinide targets were bombarded with 55-MeV α particles delivered by the 88-Inch Cyclotron at Lawrence Berkeley National Laboratory. Data was collected for 17.7 h on the ^{235}U target, 21.7 h on the ^{236}U target, and 43.5 h on the ^{239}Pu target. Emitted particles and fission fragments were detected in the Silicon Telescope Array for Reaction Studies (STARS) [23]. The STARS array is comprised of a series of double-sided, annular Si detectors for particle detection. Each detector is segmented into 48 rings and 16 sectors; adjacent rings and sectors are combined for a total of 24 rings and 8 sectors. For this study, the array consisted of two detectors downstream of the target for reaction channel identification, and a third detector, upstream from the target, for fission tagging.

The downstream detectors consisted of 150 and 1003-μm thick detectors, respectively. This telescope array covered a range of 31° to 61° at forward angles, relative to the beam axis. A 12.5-μm thick aluminum shield was placed in front of the telescope array to stop scattered fission fragments and to protect the Si detectors from δ electrons emitted from the target. The silicon telescope effectively detected hydrogen (p,d,t) and helium (^{3}He, α) species emitted in the reaction.

The third detector, 140 μm thick, was placed 8.9-mm upstream of the target for fission tagging. This detector subtended angles of 142° to 165° relative to the beam axis. The deposited energy was used to delineate fission events; an example spectrum is shown in Fig. 3. In addition, a time-to-amplitude converter (TAC) between a fission hit and a coincidence detected in both downstream detectors was used to select prompt fission events. The particle-fission TAC for the ^{239}Pu target is shown in Fig. 4.

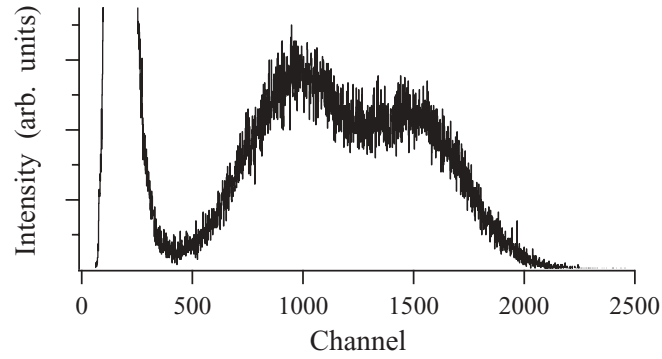

FIG. 3. Fission spectrum observed with the ^{239}Pu target, in coincidence with prompt α particles detected in the downstream detectors. The low energy peak is largely due to the large flux of α particles emitted with the natural radioactive decay of the target. Fission events are above channel 500.

IV. RESULTS

In total, 1.1 $\times 10^5$ background-subtracted prompt α-fission coincidence events were observed with the ^{239}Pu target. The surrogate ratio targets of ^{235}U and ^{236}U resulted in 3.5 $\times 10^4$ and 8.6 $\times 10^4$ coincidence events, respectively. The coincidence yield, as a function of α energy, is shown in Fig. 5.

For each target, the equivalent neutron energy is determined from the difference between the nuclear excitation energy and the neutron separation energy. The ratios of α-fission coincidence events at each neutron energy, corrected for experimental properties as shown in Eq. (5), are shown in Fig. 6 for each target.

The uncertainty in neutron energy for each data point is approximately 108 keV. Contributions to the uncertainty are similar to those outlined in Ref. [16], and are shown in Table II. The energy straggle of the α particles passing through the target and the detector components, as well as the angle of emission incur an uncertainty of $\sim$44 keV. The intrinsic

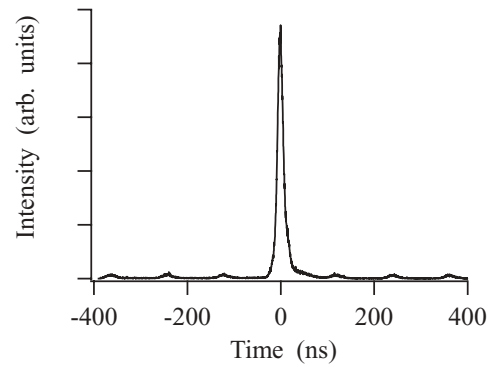

FIG. 4. α-particle-fission TAC spectrum observed with the ^{239}Pu target. The full width at half maximum (FWHM) for the prompt peak is 18.4 ns. The periodic structure of the random particle-fission events is due to the 8.2602-MHz-cyclotron frequency.

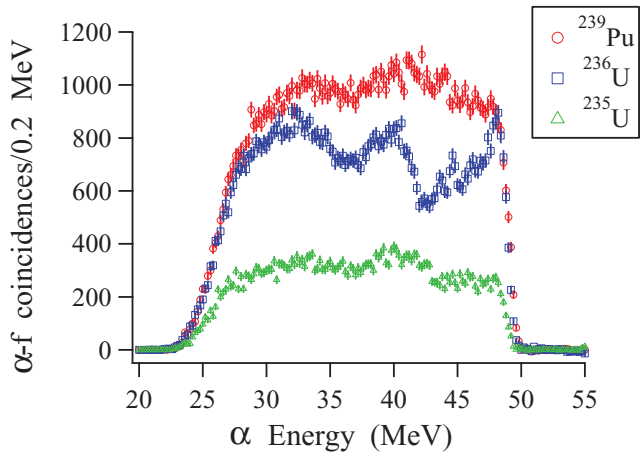

FIG. 5. (Color online) Background-subtracted α-fission coincidences as a function of α energy for each target used in the current experiment. First- , second-, and third-chance fission peaks can be observed.

detector resolution of ∼77 keV was determined from a ^{226}Ra source measurement immediately preceding and following the reaction experiment. The uncertainty of the cyclotron energy has been estimated at 60 keV for a 55-MeV α beam [16].

As the same experimental conditions existed for all three target species, the fission detection efficiencies cancel in the SRM. This assumption was validated by the ratio of fission fragment anisotropies, shown in Fig. 7. The anisotropy was defined as the number of "in-plane" fission events divided by the number of "out-of-plane" events. The reaction plane was determined by the scattered α particle; fission events in the same or opposite sector number as the α particle are within the reaction plane. Fission events in sectors orthogonal to the reaction plane comprised the out-of-plane events. While the fission anisotropy varies as a function of neutron energy, the ratios are equal within the experimental uncertainties over the energy range of interest.

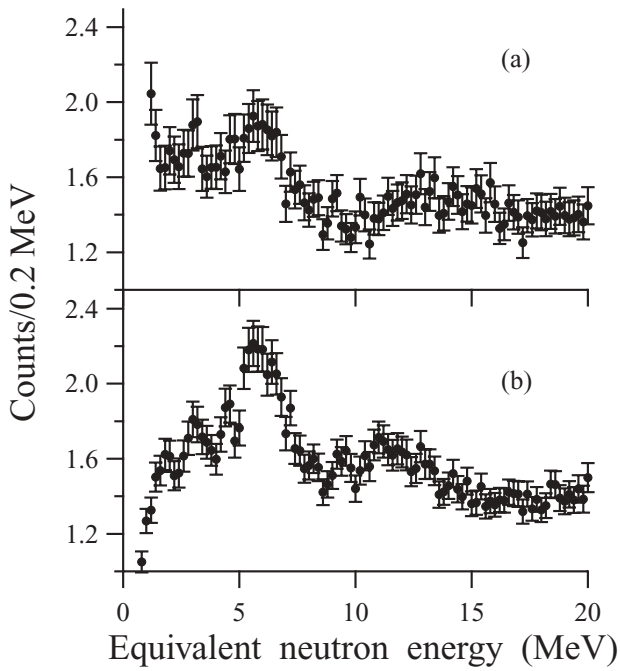

FIG. 6. Coincidence ratios, corrected for experimental parameters, for the two ratio surrogate reactions. Panel (a) shows the ratio for ^{239}Pu/^{235}U and (b) shows the ratio for ^{239}Pu/^{236}U.

TABLE II. Systematic sources of energy uncertainty.

Source	ΔE (keV)
α energy straggle in target and δ shield	26–49
Recoil angle	11–34
Intrinsic detector resolution	60–94
Cyclotron beam	60
Total	89–126

The experimental ratios shown in Fig. 6 must be multiplied by the respective formation (σ_{CN}) and reference ($\sigma_{(n,f),\mathrm{ref}}$) cross sections to yield the ^{238}Pu(n,f) cross section under the Weisskopf-Ewing assumption. The formation cross sections, shown in Fig. 8, were calculated using the optical-model potential Flap2.2, described in the Appendix of Ref. [24]. The neutron-induced fission reference cross sections were calculated using the statistical reactions code STAPRE [25], as outlined in Refs. [22,24]. Discrete levels and γ branching ratios were taken from the recent RIPL-3 evaluation [26], and the parameters were updated. The calculated (n,f) cross sections are in close agreement with recent evaluations, as shown in Fig. 9, and reproduce current data sets well. The resulting ^{238}Pu(n,f) cross sections are shown in Fig. 10 for the ^{234}U(n,f) and ^{235}U(n,f) reference reactions.

Both surrogate ratio measurements yield similar results for neutron energies above 5 MeV. The ^{238}Pu(n,f) cross section is observed to vary little with energy, exhibiting a cross section of approximately 3 b from 5 to 20 MeV. Below 5 MeV, differences are observed. The discrepancy is related to the breakdown of the Weisskopf-Ewing approximation that underlies the surrogate ratio approach employed here.

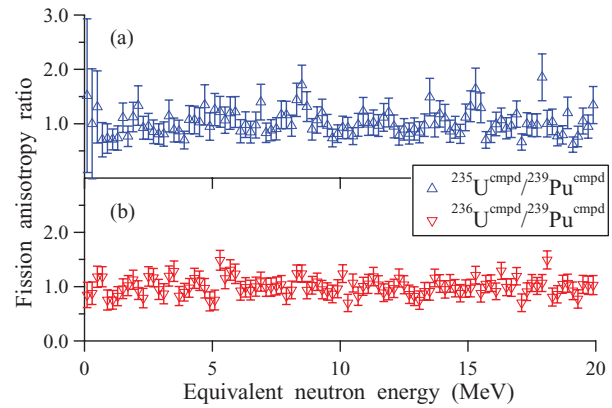

FIG. 7. (Color online) (Color online) Fission fragment anisotropy ratios for each target used in the experiment. The anistropy of the (a) ^{235}U compound nucleus is shown relative to ^{239}Pu, and of the (b) ^{236}U relative to ^{239}Pu. The values scatter about unity, confirming the cancellation of fission detector efficiencies in Eq. (4)

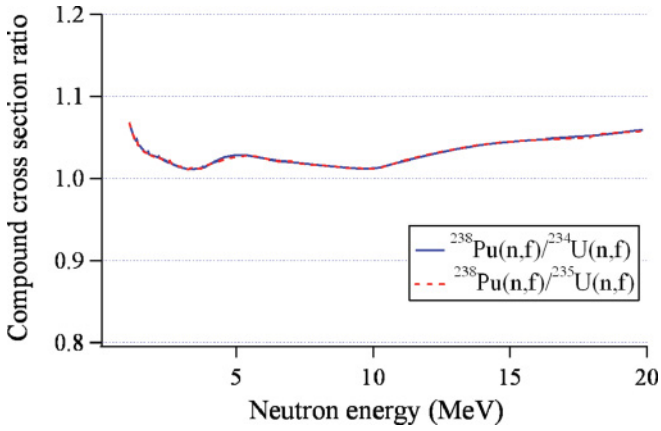

FIG. 8. (Color online) Ratio of compound nuclear formation cross sections for ^{238}Pu(n,f) relative to ^{234}U(n,f) and ^{235}U(n,f).

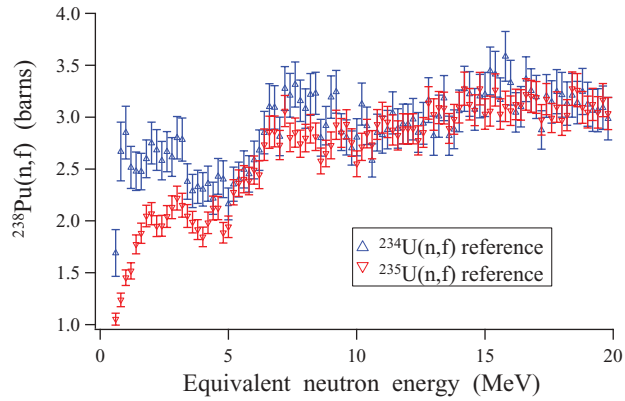

FIG. 10. (Color online) Neutron-induced fission cross sections of ^{238}Pu using two surrogate ratio measurements.

The observed differences at low energy are expected, based on theoretical studies [22] and experimental tests of the ratio approach [12,17]. The expectations were confirmed by simulating the effect of the spin-parity mismatch on the present results. The slight difference near second-chance fission ($\sim$7 MeV) is also attributed to spin effects. A significant amount of experimental data exists for neutron energies below 5 MeV, and the current work focuses on obtaining the ^{238}Pu(n,f) cross section for energies between 5 and 20 MeV, where the SRM is valid.

The observation that both measurements yield similar cross section results for neutron energies above 5 MeV can be taken as an additional indication of the validity of the ratio approach. Inelastic α scattering on ^{236}U and ^{239}Pu is expected to produce similar spin-parity distributions in the compound nuclei, as the targets' ground states have $J^{\pi} = 0^{+}$ and $1/2^{+}$, respectively. Inelastic α scattering on ^{235}U and ^{239}Pu, on the other hand, is expected to produce different spin distributions in the relevant compound nuclei, as the ground state of ^{235}U is $J^{\pi} = 7/2^{-}$. While this does not account for the fact that these spin distributions are expected to be different from those populated in the desired reaction, it is an indication that the Weisskopf-Ewing limit is approximately valid and that the ratio approach reduces potential discrepancies due to deviations from this limit.

A comparison of the surrogate data to direct measurements is shown in Fig. 11. Below 5 MeV, the current data deviates from previous results, as expected, due to the limit of the Weisskopf-Ewing approximation as discussed above. Above 5 MeV, the current data agree very well with the more recent measurement of Ref. [5] in the 5–10 MeV energy range. Near 15 MeV, the surrogate data lies higher than the earlier measurements, although the difference is less than 20%.

The surrogate data presented here provides continuous data from 5 to 20 MeV using two independent reference reactions; this data was used to perform a calculation for the ^{238}Pu cross section in a manner similar to the ^{234}U(n,f) and ^{235}U(n,f)

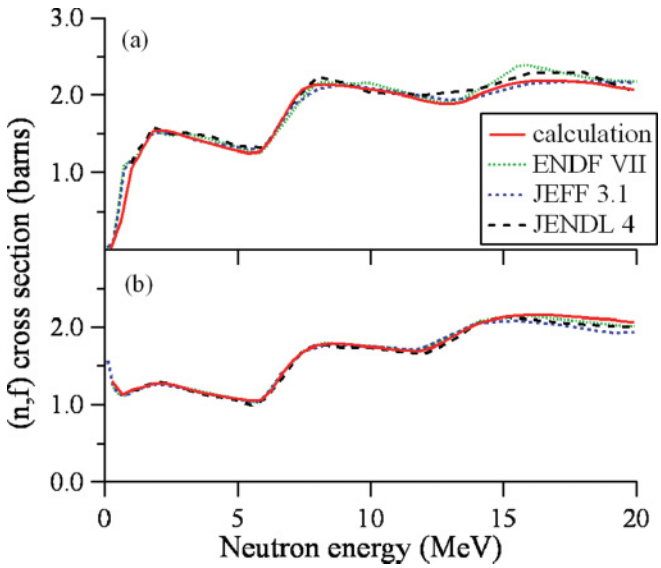

FIG. 9. (Color online) Calculated values for neutron-induced fission cross sections compared to standard data libraries for (a) ^{234}U(n,f) and (b) ^{235}U(n,f).

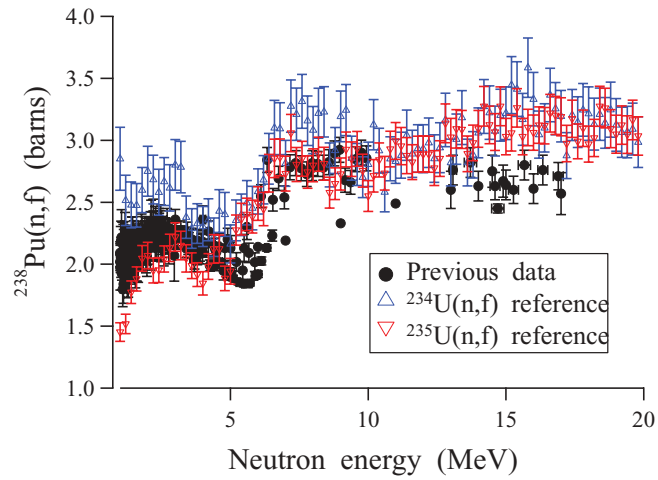

FIG. 11. (Color online) Current and previous neutron-induced fission cross sections for ^{238}Pu above 1 MeV neutron energy. Previous data are from Refs. [4–11].

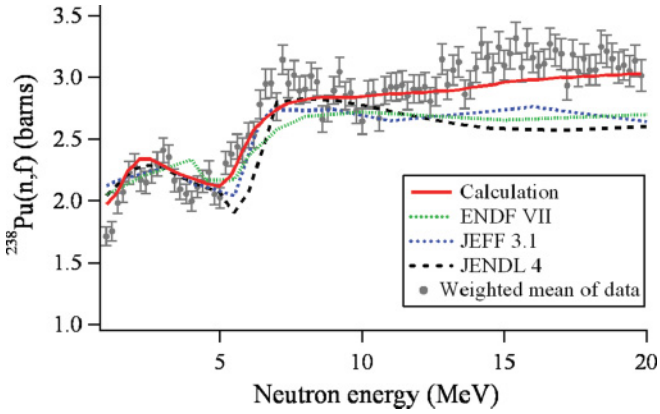

FIG. 12. (Color online) Neutron-induced fission cross sections for ^{238}Pu from selected data libraries and a new calculation considering the current data. Also shown are the weighted average data points from the two surrogate reactions. Note that the data and evaluation agreement below 5 MeV is coincidental as the two surrogate reactions employed here resulted in opposite angular momentum effects at low energy.

reactions described above. The new calculation is shown in Fig. 12 with the standard data libraries and a weighted average of the surrogate data. Below ∼10 MeV, the new result agrees well with the published libraries. Above this energy, a higher cross section is proposed, in accordance with the new experimental results.

TABLE III. Cross-section data needed for next-generation reactor technologies for neutron energies greater than 1 MeV and required accuracy ⩾5% derived from Ref. [27]. Potential surrogate reactions and ratios are also shown. An x denotes a light charged particle, such as a p, d, t, α, or ^{3}He. Only target species with half-lives greater than 5000 yr were considered.

Reaction	Surrogate	Ratio	Ratio Surrogate
^{241}Pu(n,f)	^{242}Pu$(x,x'f)$	^{235}U(n,f)	^{236}U$(x,x'f)$
	^{244}Pu(p,tf)	^{235}U(n,f)	^{238}U(p,tf)
	^{244}Pu(p,tf)	^{239}Pu(n,f)	^{242}Pu(p,tf)
	^{238}U(^{6}Li,df)	^{235}U(n,f)	^{232}Th(^{6}Li,df)
^{241}Am(n,f)	^{240}Pu(^{3}He,pf)	^{237}Np(n,f)	^{236}U(^{3}He,pf)
	^{242}Pu(^{3}He,tf)	^{237}Np(n,f)	^{238}U(^{3}He,tf)
	^{240}Pu(^{6}Li,αf)	^{237}Np(n,f)	^{236}U(^{6}Li,αf)
^{242}Am(n,f)	^{243}Am$(x,x'f)$	^{234}U(n,f)	^{235}U$(x,x'f)$
^{243}Cm(n,f)	^{245}Cm(p,df)	^{233}U(n,f)	^{235}U(p,df)
	^{245}Cm(d,tf)	^{233}U(n,f)	^{235}U(d,tf)
	^{245}Cm(^{3}He,αf)	^{233}U(n,f)	^{235}U(^{3}He,αf)
	^{242}Pu(^{6}Li,df)	^{235}U(n,f)	^{232}Th(^{6}Li,df)
	^{239}Pu(^{6}Li,pf)	^{239}Pu(n,f)	^{235}U(^{6}Li,pf)
^{244}Cm(n,f)	^{245}Cm$(x,x'f)$	^{234}U(n,f)	^{235}U$(x,x'f)$
	^{247}Cm(p,tf)	^{239}Pu(n,f)	^{242}Pu(p,tf)
	^{247}Cm(p,tf)	^{235}U(n,f)	^{238}U(p,tf)
^{245}Cm(n,f)	^{245}Cm(d,pf)	^{235}U(n,f)	^{235}U(d,pf)
	^{245}Cm(d,pf)	^{239}Pu(n,f)	^{239}Pu(d,pf)
	^{242}Pu(^{6}Li,df)	^{235}U(n,f)	^{232}Th(^{6}Li,df)
	^{242}Pu(^{6}Li,df)	^{239}Pu(n,f)	^{236}U(^{6}Li,df)

V. CONCLUSIONS

In summary, the neutron-induced fission cross section of ^{238}Pu was measured using the surrogate ratio method. The (n,f) cross section was deduced from α-induced fission reactions on ^{239}Pu, with ^{235}U$(\alpha,\alpha'f)$ and ^{236}U$(\alpha,\alpha'f)$ used as references. These reference reactions reflect ^{234}U(n,f) and ^{235}U(n,f) yields, respectively. Use of the SRM technique to determine actinide cross sections reduces the effects of contaminants, such as target backing materials and impurities. The two reactions should involve targets with similar nuclear structure characteristics, such as ground-state spins and parities and neutron separation energies. However, as previous [17] and current work shows, for higher neutron energies, the differences do not play a significant role for isotopes near one another in mass and proton number.

The uncertainty for the ^{238}Pu(n,f) cross section is ∼5% over the range 5–20 MeV using ^{235}U(n,f) as the reference reaction. For the ^{234}U(n,f) reference, the uncertainty is modestly higher at ∼7%. In many cases, this uncertainty is adequate for reactor applications and transmutation schemes.

Table III highlights fast neutron reaction data needed, where the required accuracy can likely be attained through surrogate reaction work. Candidate reactions for surrogate ratio measurements are also shown.

For the ^{241}Pu surrogate measurement, higher-mass Pu isotopes may be used. These isotopes, with longer half-lives than 14.1-yr ^{241}Pu, will still be quite active. Use of these isotopes will require careful experimental conditions to reduce the background effects from the decay of the target material. Recently, the ^{241}Pu cross section has been measured directly using neutron time of flight [28]. Uncertainties of less than 1% are reported for the 10–20 MeV neutron range. Differences with standard libraries exceed 30% in some energy ranges, and confirmatory measurements are warranted.

The ^{241}Am, ^{242}Cm, and ^{243}Cm fission cross sections have been recently measured at low energy (<10 MeV for ^{241}Am and ^{242}Cm, <3.2 MeV for ^{242}Cm) using ^{243}Am(^{3}He,x) surrogate reactions, where x is a deuteron, triton, or α particle [29]. This work reports uncertainties ∼11–14%; these uncertainties could be lessened with higher-statistics data and the reaction could be used to extend the cross-section measurement to higher energies.

ACKNOWLEDGMENTS

The authors thank the 88-Inch Cyclotron operations and facilities staff for the support of this study. We would also like to thank the Department of Energy's NNSA, Office of Nonproliferation Research and Development (NA-22), for financial support. This work was performed under the auspices of the US Department of Energy under Contracts No. DE-AC52-07NA27344 (LLNL) and No. DE-AC02-05CH11231 (LBNL).

[1] Spiegel Online, 25 January 2010 [www.spiegel.de/international/germany/0,1518,673875,00.html].
[2] World Nuclear News, 18 June 2010, [www.world-nuclear-news.org/NP_New_phase_for_Swedish_nuclear_1806101.html].
[3] "A Technology Roadmap for Generation IV Nuclear Energy Systems," No. GIF-002-00, Generation IV International Forum, 2002.
[4] Gu Fu-Hua, Report No. HSJ-77065, Institute of Atomic Energy, Beijing, China, 1978.
[5] C. Budtz-Joergensen, J.-H. Knitter, and D. L. Smith, *Proceedings of the International Conference on Nuclear Data for Science and Technology, Antwerp, 1982*, edited by K.-H. Böckhoff (Reidel Publishing Company, Dordrecht, 1983), p. 206.
[6] E. B. Ermagambetov and G. N. Smirenkin, Atomnaya Energiya **25**, 527 (1968).
[7] E. F. Fomushkin, E. K. Gutnikova, Ju. S. Zamyatnin, B. K. Maslennikov, V. N. Belov, V. M. Surin, F. Nasyrov, and N. F. Pashkin, Sov. J. Nucl. Phys. **5**, 689 (1967).
[8] D. M. Barton and P. G. Koontz, Phys. Rev. **162**, 1070 (1967).
[9] B. I. Fursov, B. F. Samylin, V. S. Shorin, S. A. Badikov, M. I. Svirin, E. Yu. Baranov, E. S. Lavrov, V. I. Mil'Shin, V. B. Pavlovich, S. V. Pupko, Yu. M. Turchin, and V. N. Polynov, *Proceedings of the International Conference on Nuclear Data for Science and Technology, Trieste, 1997*, edited by G. Reffo, A. Ventura, and G. Grandi (Italian Physical Society, Bologna, Italy, 1997), p. 488.
[10] M. G. Silbert, A. Moat, and T. E. Young, Nucl. Sci. Eng. **52**, 176 (1973).
[11] D. M. Drake, C. D. Bowman, M. S. Coops, and R. W. Hoff, Los Alamos Scientific Lab. Rep. No. 4420, 1970, p. 101.
[12] S. L. Lesher *et al.*, Phys. Rev. C **79**, 044609 (2009).
[13] J. D. Cramer and H. C. Britt, Nucl. Sci. Eng. **41**, 177 (1970).
[14] M. Petit *et al.*, Nucl. Phys. A **735**, 345 (2004).
[15] C. Plettner *et al.*, Phys. Rev. C **71**, 051602(R) (2005).
[16] J. T. Burke *et al.*, Phys. Rev. C **73**, 054604 (2006).
[17] B. F. Lyles *et al.*, Phys. Rev. C **76**, 014606 (2007).
[18] B. K. Nayak, A. Saxena, D. C. Biswas, E. T. Mirgule, B. V. John, S. Santra, R. P. Vind, R. K. Chowdhury, and S. Ganesan, Phys. Rev. C **78**, 061602(R) (2008).
[19] M. S. Basunia *et al.*, Nucl. Instrum. Methods Phys. Res. Sect. B **267**, 1899 (2009).
[20] J. M. Allmond *et al.*, Phys. Rev. C **79**, 054610 (2009).
[21] B. L. Goldblum *et al.*, Phys. Rev. C **80**, 044610 (2009).
[22] J. E. Escher and F. S. Dietrich, Phys. Rev. C **74**, 054601 (2006).
[23] S. R. Lesher *et al.*, Nucl. Instrum. Methods Phys. Res. Sect. A **621**, 286 (2010).
[24] J. E. Escher and F. S. Dietrich, Phys. Rev. C **81**, 024612 (2010).
[25] M. Uhl and B. Strohmaier, "Stapre, a Computer Code for Particle Induced Activation Cross Sections and Related Quantities," Technical Report No. IRK 76/01, rev. 1978, Institut für Radiumforschung und Kernphysik, Vienna, Austria, 1976.
[26] R. Capote *et al.*, Nucl. Data Sheets **100**, 3107 (2009).
[27] G. Alibertiet *al*, Ann. Nucl. Eng. **33**, 700 (2006).
[28] F. Tovesson and T. S. Hill, Nucl. Sci. Eng. **165**, 224 (2010).
[29] G. Kessedjian *et al.*, Phys. Lett. B **692**, 297 (2010).